

# Multiwavelength Monitoring of the BL Lacertae Object PKS 2155–304 in May 1994.

## I. The Ground-Based Campaign

Joseph E. Pesce<sup>1</sup>, C. Megan Urry<sup>1</sup>, Laura Maraschi<sup>2</sup>, Aldo Treves<sup>3</sup>,  
Paola Grandi<sup>4</sup>, Ronald I. Kollgaard<sup>5,6</sup>, Elena Pian<sup>1</sup>, Paul S. Smith<sup>7,8</sup>,  
Hugh D. Aller<sup>9</sup>, Margo F. Aller<sup>9</sup>, Aaron J. Barth<sup>10</sup>, David A. H. Buckley<sup>11</sup>,  
Elvira Covino<sup>12</sup>, Alexei V. Filippenko<sup>10</sup>, Eric J. Hooper<sup>7</sup>, Michael D. Joner<sup>13,14</sup>,  
Lucyna Kedziora-Chudczer<sup>15</sup>, David Kilkenny<sup>11</sup>, Lewis B. G. Knee<sup>16,17</sup>,  
Michael Kunkel<sup>18</sup>, Andrew C. Layden<sup>19,20</sup>, Antonio Mário Magalhães<sup>21</sup>,  
Fred Marang<sup>11</sup>, Vera E. Margoniner<sup>21</sup>, Christopher Palma<sup>5,22</sup>,  
Antonio Pereyra<sup>21</sup>, Claudia V. Rodrigues<sup>21,23</sup>, Andries Schutte<sup>24,25</sup>,  
Michael L. Sitko<sup>26</sup>, Merja Tornikoski<sup>27</sup>, Johan van der Walt<sup>28</sup>,  
Francois van Wyk<sup>11</sup>, Patricia A. Whitelock<sup>11</sup>, Scott J. Wolk<sup>14,29</sup>

---

<sup>1</sup>Space Telescope Science Institute, 3700 San Martin Drive, Baltimore, MD 21218. The Space Telescope Science Institute is operated by the Association of Universities for Research in Astronomy, Inc., under contract with the National Aeronautics and Space Administration.

<sup>2</sup>Osservatorio Astronomico di Brera, via Brera 28, I-20121 Milan, Italy.

<sup>3</sup>SISSA/ISAS, strada Costiera 11, I-34014 Trieste, Italy.

<sup>4</sup>IAS/CNR, via Enrico Fermi 23, CP67, I-00044 Frascati, Italy.

<sup>5</sup>Department of Astron. and Astrophys., Penn State Univ., University Park, PA 16802.

<sup>6</sup>Present address: Fermi National Accelerator Laboratory, Box 500, Batavia, IL, 60510.

<sup>7</sup>Steward Observatory, University of Arizona, Tucson, AZ 85721.

<sup>8</sup>Present address: NOAO/KPNO, P.O. Box 26732, Tucson, AZ 85726-6732.

<sup>9</sup>Department of Astronomy, University of Michigan, Ann Arbor, MI 48109-1090.

<sup>10</sup>Department of Astronomy, University of California, Berkeley, CA 94720-3411.

<sup>11</sup>SAAO, P.O. Box 9, 7935 Observatory, Western Cape, South Africa.

<sup>12</sup>Osservatorio Astronomico di Capodimonte, via Moiariello 16, I-80131 Naples, Italy.

<sup>13</sup>Dept. of Physics and Astronomy, FB, Brigham Young University, Provo, UT 84602.

<sup>14</sup>Visiting Astronomer, Cerro Tololo Inter-American Observatory, La Serena, Chile. CTIO is operated by Association of Universities for Research in Astronomy, Inc., under contract with the National Science Foundation.

<sup>15</sup>Australia Telescope National Facility, P.O. Box 76, Epping NSW 2121, Australia.

<sup>16</sup>Swedish-ESO Submillimetre Telescope, ESO, Casilla 19001, Santiago 19, Chile.

<sup>17</sup>Also with the Onsala Space Observatory, S-43992 Onsala, Sweden.

<sup>18</sup>Max-Planck-Institut für Astronomie, Königstuhl 17, 69117 Heidelberg, Germany.

<sup>19</sup>Cerro Tololo Inter-American Observatory, Casilla 603, La Serena, Chile.

<sup>20</sup>Present address: McMaster University, Dept. of Physics and Astronomy, Hamilton, ON L8S 4M1 Canada.

<sup>21</sup>Instituto Astronomico e Geofísico, Universidade de São Paulo, Caixa Postal 9638, São Paulo SP 01065-970, Brazil.

<sup>22</sup>Present address: Department of Astronomy, University of Virginia, PO Box 3818, Charlottesville, VA 22903-0818.

<sup>23</sup>Present address: Instituto Nacional de Pesquisas Espaciais-INPE Divisão de Astrofísica-DAS, Caixa Postal 515, São José dos Campos, SP 12201-970, Brazil.

<sup>24</sup>Department of Physics, University of Zululand, Private Bag X1001, Kwa-Dlangezwa 3886, South Africa.

<sup>25</sup>Present address: Siemens Telecommunications, 270 Maggs Street, Waltloo, Pretoria, South Africa.

## ABSTRACT

Optical, near-infrared, and radio observations of the BL Lac object PKS 2155–304 were obtained simultaneously with a continuous UV/EUV/X-ray monitoring campaign in 1994 May. Further optical observations were gathered throughout most of 1994. The radio, millimeter, and near-infrared data show no strong correlations with the higher energies. The optical light curves exhibit flickering of 0.2-0.3 mag on timescales of 1-2 days, superimposed on longer timescale variations. Rapid variations of  $\sim 0.01$  mag min $^{-1}$ , which, if real, are the fastest seen to date for any BL Lac object. Small (0.2-0.3 mag) increases in the  $V$  and  $R$  bands occur simultaneously with a flare seen at higher energies. All optical wavebands ( $UBVRI$ ) track each other well over the period of observation with no detectable delay. For most of the period the average colors remain relatively constant, although there is a tendency for the colors (in particular  $B - V$ ) to vary more when the source fades. In polarized light, PKS 2155–304 showed strong color dependence (polarization increases toward the blue,  $P_U/P_I = 1.31$ ) and the highest optical polarization ( $U = 14.3\%$ ) ever observed for this source. The polarization variations trace the flares seen in the ultraviolet flux. For the fastest variability timescale observed, we estimate a central black hole mass of  $\lesssim 1.5 \times 10^9 (\frac{\delta}{10}) M_\odot$ , consistent with UV and X-ray constraints and smaller than previously calculated for this object.

*Subject Headings:* BL Lacertae objects: individual (PKS 2155–304) — galaxies: active — galaxies: photometry — polarization

## 1. Introduction

Among active galactic nuclei (AGNs) the blazar class (BL Lacertae objects and violently variable quasars) is known for rapid variability, high luminosity, and high level of polarization. The observed properties of blazars are currently interpreted as nonthermal (synchrotron and inverse Compton) emission from an inhomogeneous relativistic jet oriented close to the line of sight (Blandford & Rees 1978). Typical jet models (Ghisellini, Maraschi,

---

<sup>26</sup>Department of Physics, University of Cincinnati, Cincinnati, OH 45221-0011.

<sup>27</sup>Metsahovi Radio Research Station, Metsahovintie 114, FIN-02540 Finland.

<sup>28</sup>Space Research Unit, Potchefstroom University, Potchefstroom 2520, South Africa.

<sup>29</sup>SUNY, Stony Brook, New York 11794-2100.

& Treves 1985; Marscher & Gear 1985; Königl 1989) have a large number of free parameters and are underconstrained by single epoch spectral distributions. Combining spectral and temporal information greatly constrains the jet physics, since different models predict different variability as a function of wavelength. Elucidating the structure of blazar jets through multiwavelength monitoring and polarization studies is an essential precursor to understanding their formation and thus the extraction of energy from the central engine.

At low frequencies (radio-mm-infrared-optical) this technique has already led to substantial progress: the evolution of radio flares in time and frequency has been used to deduce the structure of the outer parts of the jet (Hughes, Aller, & Aller 1989). The variations among the radio bands are well correlated and lags are typically weeks to months. In some cases, optical variations precede radio ones by about a year, although only weak correlations have been established (Bregman & Hufnagel 1989). Some blazars also exhibit intraday variability at optical and radio wavelengths (Wagner & Witzel 1995, and references therein). Optical polarimetry shows that the synchrotron continuum completely dominates the emission from most blazars at optical and ultraviolet wavelengths (Smith & Sitko 1991). While variations are present at all frequencies, blazars are generally most variable at the shortest wavelengths (optical, UV, X-ray).

The BL Lac object PKS 2155–304 is an excellent candidate for blazar monitoring because it is both rapidly variable and bright enough that its variability can be resolved at wavelengths shorter than optical (Edelson et al. 1995); in particular, PKS 2155–304 is one of only two blazars (the other being Mrk 421) that can be monitored sufficiently rapidly with the *International Ultraviolet Explorer* (*IUE*) satellite. It is also one of the brightest extragalactic sources detected with the *Extreme Ultraviolet Explorer* satellite (*EUVE*; Marshall, Carone, & Fruscione 1993; Fruscione et al. 1994). PKS 2155–304 is one of the strongest X-ray emitters and is a typical X-ray selected BL Lac object.

High energy  $\gamma$ -rays from PKS 2155–304 have been detected recently by the EGRET experiment on board the *Compton Gamma-Ray Observatory* (*CGRO*; Vestrand, Stacy, & Sreekumar 1995), confirming that the emission processes in PKS 2155–304 are similar to those in the many blazars already detected with *CGRO*. Thus, by studying multiwavelength variability in this bright and highly variable object, we derive information relevant for the whole class, especially for the “high-frequency peaked BL Lacs” (Padovani & Giommi 1995), i.e., X-ray selected BL Lacs.

Attempts at multiwavelength studies of PKS 2155–304 with *IUE* and *EXOSAT* (Treves et al. 1989) indicated a correlation of the two wavebands but also the need for much better sampling. Multiwavelength monitoring of PKS 2155–304 in 1991 November (Smith et al. 1992; Urry et al. 1993; Brinkmann et al. 1994; Courvoisier et al. 1995; Edelson

et al. 1995) produced the best available data for any blazar. This soft X-ray/UV/optical monitoring of PKS 2155–304 found the emission at these wavelengths was well correlated, that there was significant short timescale variability (< 1 day), and that the X-ray flux led the ultraviolet by a few hours. The tight X-ray/UV correlation and the overall UV to X-ray spectral shape confirmed the supposition that synchrotron emission is responsible for the optical-through-X-ray continuum in this BL Lac object (and presumably in others with similar spectra and variability), and ruled out conclusively any observed optical/UV continuum from an accretion disk (as argued also on the basis of polarization studies in the optical/UV). However, this campaign had sufficient sampling only over a short period of time (4 days).

For this reason a second campaign was organized in 1994 May where the intensive *IUE* monitoring was extended to 10 days. The ultraviolet, extreme ultraviolet, and X-ray observations, as well as the overall multiwavelength campaign, are addressed elsewhere (Pian et al. 1996; Marshall et al. 1996; Kii et al. 1996; Urry et al. 1996). Here we discuss the ground-based observations during the 1994 May campaign and beyond.

This paper is organized as follows. In Section 2 we present the ground-based observations made from 1994 May through 1994 November. Section 3 includes a discussion of these data, and conclusions are given in Section 4.

## 2. Multiwavelength Ground-Based Observations

### 2.1. Radio

The Very Large Array (VLA)<sup>30</sup> was used in a hybrid A/B configuration to monitor the arcsecond core of PKS 2155–304 on 12 days (1994 May 14 - June 1) at 3 frequencies (8.4, 15.0, and 22.5 GHz), with 1.5 and 5.0 GHz measurements also taken on four of these occasions (see Table 1). Standard frequency settings and dual 50 MHz bandwidths were used. The uncertainties listed in the Table are the internal errors and do not include systematic effects, which will alter the overall flux scale (see below).

Observations of a few minutes were made at each frequency with similar but not identical *uv*-coverage on the different days. Complementary observations (once per day at each frequency) were also made of 3C 48 and one or both of two nearby calibrator sources

---

<sup>30</sup>The National Radio Astronomy Observatory is operated by Associated Universities, Inc., under cooperative agreement with the NSF.

(2151–304, 2248–325) which we assumed to be non-variable. Due to poor *uv* coverage of 3C 48, standard VLA calibration techniques failed, and we determined the flux densities directly from the raw *uv* data. The absolute flux scale is therefore dependent upon the overall gain normalization applied to the data during calibration and should be accurate to 10% at 22.5 GHz and 5% at the four lower frequencies (R. A. Perley, private communication). However, the flux densities obtained from 3C 48 and the calibrator sources show that the relative flux scale is better than this, with variations of 1%, 1%, 3%, 3%, and 4% noted at 1.5, 5, 8.4, 15, and 22.5 GHz, respectively. At all frequencies PKS 2155–304 was more variable than the calibrator sources. The data collected on May 26 (MJD 9499.05)<sup>31</sup> were systematically low for all sources and have been scaled by assuming that the calibrators are non-variable.

Data at three frequencies (4.8, 8, and 14.5 GHz) were also obtained with the University of Michigan Radio Astronomy Observatory (UMRAO) 26 m single-dish telescope (Table 2). The observational technique and reduction procedures are discussed by Aller et al. (1985). Typically, each daily observation consists of a series of on-off measurements over a 30 to 45 minute time period. The flux scale is based on observations of 3C 461 and the absolute scale of Baars et al. (1977). This primary standard, or a nearby secondary flux standard (one of 3C 58, 3C 144, 3C 145, 3C 218, 3C 274, 3C 286, 3C 353, or 3C 405), was routinely observed every 1.5 to 2 hours to correct for time-dependent variations in the gain of the instrument. There is a 5% uncertainty in the final flux density scale.

Further radio observations were obtained with the Australia Telescope Compact Array (ATCA; Frater, Brooks, & Whiteoak 1992), at the Australia Telescope National Facility, on 1994 May 4–5, May 19–22, and August 30–31. PKS 2155–304 was monitored as part of a program to search for intraday variations in a sample of quasars and BL Lac objects. The ATCA consists of six 25 m antennas arranged in an east–west line and observations were done at four wavelengths (3, 6, 13, and 20 cm). Two slightly different configurations were used throughout the monitoring, 6A and 6D, with maximum baselines 5939 m and 5878 m, respectively. The data were taken at 3 and 6 cm simultaneously, then at 13 and 20 cm after rotating the turrets. The correlator was configurated in the standard way with 32 channels across a bandwidth of 128 MHz for each wavelength. During the monitoring program the source was scanned four times every 24 hours, on average. Each scan lasted one minute with integration times of 10 seconds. A turret was rotated between two pairs of wavelengths every second minute to provide almost simultaneous coverage of the available radio spectrum, with two orthogonal linear polarizations being measured.

The flux density scale was set on the standard primary calibrator used at ATCA, PKS

---

<sup>31</sup>In this paper, MJD is defined as JD - 2,440,000.

1934–638. The changes in phase caused by the receiver, local oscillator, and atmosphere were calibrated on the nearby point source (the secondary calibrator), PKS 2149–307. The flux densities given in Table 3 are the averages over all 13 baselines, with the exception of the two shortest baselines in order to reduce the influence of the extended structure of PKS 2155–304 and other confusing sources in the field. This is particularly important at 20 cm where the size of the primary beam is the largest (33 arcmin).

## 2.2. Millimeter

Observations were made using the 15 m Swedish-ESO Submillimetre Telescope (SEST)<sup>32</sup>, located on La Silla, Chile (Booth et al. 1989), with the SEST facility bolometer. PKS 2155–304 was observed on 1994 May 19 and May 21 at 94 GHz and on 1994 April 24–25 and June 1, 25, and 26 at 90 and 230 GHz (Table 4). Uranus was used as the primary flux calibrator and was checked by the secondary calibrator, Jupiter.

## 2.3. Optical and Near-IR Photometry, Polarimetry, and Spectroscopy

We arranged considerable observational coverage, but bad weather at several sites prevented the almost continuous level originally planned. The difficulty of obtaining continuous optical/near-infrared monitoring from the ground was exacerbated by the fact that the object was  $\sim 90^\circ$  from the sun in May, as required for the space-based observations. After May, weather and sun-angle conditions improved and monitoring observations continued to 1994 November.

Table 5 lists the 20 optical and near-infrared observers and telescopes contributing to this campaign. Limited near-infrared data were available during the middle of the campaign and are given in Table 6. Exposure times were typically  $\sim 40$  s for *JHK* and  $\sim 40$ –160 s for *L*. Observations by M. Kunkel were in the ESO IR system and have been converted to the SAAO system following Carter (1990). For the optical data (Table 7), instrumental magnitudes were converted to *UBVRI* magnitudes (Johnson *UBV* and Cousins *RI* filters) using calibration stars in the field (Hamuy & Maza 1989; Smith, Jannuzi, & Elston 1991). Typical exposure times were 60–120 s (*U*), 20–600 s (*B*), 30–300 s (*V*), 20–300 s (*R*), and 30–120 s (*I*), and the errors are in the range  $\lesssim 0.01$  to  $\sim 0.08$  mag with 0.01 mag being

---

<sup>32</sup>The Swedish-ESO Submillimetre Telescope, SEST, is operated jointly by ESO and the Swedish National Facility for Radio Astronomy, Onsala Space Observatory at Chalmers University of Technology.

a typical value. Some of our observations were obtained at relatively high airmass, and the differential photometry does not adequately address the 2nd order extinction term. However, this term should account for no more than 0.03 mag.

Optical polarization measurements of PKS 2155–304 were made between 1994 May 13 and May 21 (MJD 9485-9493) using the Two-Holer polarimeter/photometer (Table 8). The instrument, observational procedures, and data reduction are described in detail by Smith et al. (1992). An 8 arcsec circular aperture was used for all of the polarimetry, and typical exposure times were three to eight minutes.

Optical polarimetry of PKS 2155–304 was also performed by the group at the University of São Paulo (USP) with their CCD Imaging Polarimeter (Table 9). The instrument was used at the Laboratorio Nacional de Astrofisica (LNA), Brazopolis, with the LNA 1.60 m and USP 0.61 m telescopes, and is described in detail by Magalhães et al. (1996). Measurement errors are consistent with photon noise. Instrumental Stokes Q,U values were converted to the equatorial system from standard star data obtained on the same night. The instrumental polarization was measured to be less than 0.03%; being considerably smaller than the measured errors, no correction has been applied to the data.

Optical spectra of PKS 2155–304 were obtained in morning twilight on 1994 June 3 (MJD 9506.9875) with the Kast double spectrograph (Miller & Stone 1993) at the Cassegrain focus of the Shane 3 m reflector at Lick Observatory. Reticon  $400 \times 1200$  pixel CCDs were used in both cameras. A long slit of width 4 arcsec was oriented along the parallactic angle to minimize differential light losses produced by atmospheric dispersion. Several different grating and grism settings were required to cover the entire accessible wavelength range (3220-9908 Å) with a resolution of 8-11 Å. The standard stars BD+26°2606 (Oke & Gunn 1983) and Feige 34 (Massey et al. 1988) were used for flux calibration. These were also used to eliminate (through division) the telluric absorption bands in the spectrum of PKS 2155–304. The atmospheric seeing during the observations was poor and variable ( $\sim 3$  -  $4''$ ). Moreover, the extinction correction cannot be fully trusted because the airmass was high (3.0-3.2). Thus, although the night was clear, the derived absolute flux for the final spectrum might be somewhat erroneous. The relative flux calibration, on the other hand, should be more reliable, except perhaps at the near-UV wavelengths.

### 3. Results and Discussion

### 3.1. Radio Results

The radio fluxes show evidence of variability at the level of a few percent at all frequencies (see Figure 1), and are better sampled than during the previous campaign in 1991 November when the flux increased by 20% in one month (Courvoisier et al. 1995). The trend in the high frequency data (22.5, 15, 8.4 GHz) is an increase of about 10% from May 14 until around May 24 (MJD 9487 - 9497) when the flux begins to decline. This trend may also be present in the less-well sampled 5 GHz data, though probably not at 1.5 GHz. The variability amplitude appears to increase with increasing frequency, from  $\sim 10\%$  to  $\sim 20\%$  for the 8.4 to 22.5 GHz data, and the peak at 8.4 and 15 GHz appears to occur simultaneously, while the 22.5 GHz peak seems to have occurred about five days earlier. There is no discernable change in the radio spectral index, unlike the case in the previous campaign where the radio spectrum flattened over the period of observation (Courvoisier et al. 1995). The large 22.5 GHz peak on May 26 (MJD 9499.05) is probably an artifact due to calibration uncertainties. The Michigan data do not show the same behavior because of the lack of coverage.

The lower frequency radio data (ATCA) show no variability over the three periods of observation. Variations of 20% would have been observed easily but are not seen (Figure 2). PKS 2155–304 does increase in brightness by 20-40% from early May to late August at all four wavelengths. Although by a smaller factor, this corresponds to the general brightening of the source in the optical over the same period (see below). A marked change in spectral index is observed for these data, with the spectrum inverting from early May to mid May and flattening by the last observations in late August. During the SEST observations the source remained invariant within the errors (Figure 3). However, variations of  $\sim 30\%$  could be present in the data, comparable to the radio and optical variations.

### 3.2. Optical and Near-IR Results

#### 3.2.1. Photometry and Variability

The near-infrared flux of PKS 2155–304 increased nearly monotonically by  $\sim 0.2$ - $0.3$  mag over a period of seven days in all observed bands (Figure 4), during the ultraviolet flaring period (Pian et al. 1996). The low  $L$  magnitude is probably spurious and has much larger errors ( $\sim 0.6$  mag) than the other measurements. The dip seen in  $H$  and  $J$  may be real, but instrumental effects cannot be excluded.

Figure 5 shows the optical ( $UBVRI$ ) light curves for PKS 2155–304 during 1994 May.

The durations of the X-ray, extreme ultraviolet, and ultraviolet campaigns (*ASCA*, *EUVE*, and *IUE*) are shown at the top (the middle of each flare is also indicated). While the coverage is sparse, general trends are the same in all wavebands. The sharp increase of 0.3 mag in the *V*-band flux, and to a lesser extent in the *R*-band flux, between MJD 9492 and 9494 corresponds to the flare seen in the ultraviolet at the same period (Urry et al. 1996). This increase does not seem present in the *B* band (unless earlier), and there is no simultaneous data in the *U* or *I* bands.

The entire April - November light curve for PKS 2155–304 is shown in Figure 6. There is a general “flickering” (mini-flares of  $\sim$ 0.2-0.4 mag in several days) of the source in all bands throughout this period, superimposed on a general, slow brightening (0.4-0.7 mag) through September, followed by a 0.4 - 0.7 magnitude drop between the last observations in September (MJD 9608) and the final observations in November (MJD 9672). Throughout the observation period, PKS 2155–304 was brighter than the average ( $B = 13.58$ ) seen by Pica et al. (1988) over the period 1979-1986. In early June (MJD  $\sim$ 9500-9520), a large flare is seen in all observed optical bands. The amplitude of this feature is 0.3 - 0.4 mag with a rise time of about 10 days and a duration of about 20 days, although it may not be resolved.

The largest observed excursions are a drop in the *B* band of  $\sim$  0.5 mag in 4 days and almost a magnitude in *U* in about 10 days, both in May, right at the start of the multiwavelength observing campaign (MJD 9475 - 9484, Figure 5). The other bands exhibit a drop in magnitude over this period, but of much smaller amplitudes ( $\sim$ 0.2 mag). There are no UV or X-ray data during this period; the drop in flux in the 4.8 GHz band is possibly correlated with the drop in the *U* band, though this is most likely coincidental.

The fastest variations are changes of 0.1-0.2 mag in tens of minutes. An example of this is the *I*-band flux at MJD  $\sim$ 9486 (Figure 5), which increases by 0.18 mag in 13.5 minutes ( $\sim$ 0.01 mag min $^{-1}$ !), corresponding to a doubling time of 75 minutes; a lesser increase is also seen in the *B* and *R* bands. Several such increases are seen in the other bands over the observation period. In fact, if real, these are the fastest optical variations seen for any BL Lac (by about a factor of five; for OQ 530, Carini, Miller, & Goodrich 1990 observed an increase of 0.06 mag in 20 minutes). A timescale of about an hour is consistent with the results of a structure analysis of several nights of photometry by Paltani et al. (1996), who found that the minimum timescale of variations is shorter than 15 minutes. The other variations we observe,  $\sim$ 0.01 mag hour $^{-1}$  or several tenths of a magnitude over days, have been seen before in PKS 2155–304 (Carini & Miller 1992) and are typical for these objects (e.g., BL Lac, OJ 287, Miller, Carini, & Goodrich 1989; Carini et al. 1992; 0235+164, Rabbette et al. 1996; 0716+714, Wagner et al. 1996). The blazar 3C 279, the subject of a

similar multiwavelength campaign, was seen to double its  $R$ -band flux in 10 days (Grandi et al. 1996).

The most rapid variations observed give us a minimum doubling time or variability timescale,  $t_D = 75$  min. This, in fact, may not be a doubling timescale since we have not observed a true doubling of the flux. Nonetheless, we can estimate an upper limit to the black hole mass if we assume that these variations are caused by radiation generated close to a supermassive black hole (at  $R = 3R_s$ , where  $R_s = 2GM/c^2$  is the Schwarzschild radius), and that the emission is isotropic. An estimate of the upper limit to the size of the emitting region is  $R \approx \delta ct_D$ , where  $\delta$  is the Doppler factor which takes relativistic beaming into account;  $\delta \sim 10$ .

The limit to the mass of the black hole can be estimated by

$$M_{\text{var}} \approx \frac{Rc^2}{6G} \lesssim \frac{\delta c^3 t_D}{6G}.$$

For PKS 2155–304 we calculate  $M_{\text{var}} \lesssim 1.5 \times 10^9 (\frac{\delta}{10}) M_\odot$ , consistent with constraints based on UV and X-ray observations (Morini et al. 1986; Urry et al. 1993), and considerably smaller than what was found by Carini & Miller (1992), taking into account the relativistic beaming term.

### 3.2.2. Colors and Spectral Shape

In general, the optical light curves of PKS 2155–304 track each other well. No lags are detected, although because of poor sampling we may be insensitive to lags of several days in many cases. The  $B - V$  and  $V - I$  colors of PKS 2155–304 were calculated from simultaneous or nearly simultaneous measurements (the majority are within one to five minutes, and eight are within 10–40 minutes). During 1994 May, the  $B - V$  colors varied from 0.2 to 0.5 mag, but for most of the rest of the observation period, they were near the average value of  $\langle B - V \rangle = 0.32 \pm 0.02$  mag. Except for three points in early May, the  $V - I$  colors were nearly constant at  $\langle V - I \rangle = 0.69 \pm 0.01$  mag (Figure 7, top panel).

The largest color variations occurred when PKS 2155–304 was faint ( $V \gtrsim 12.7$ ). For  $V < 12.7$ , the standard deviation of the  $B - V$  colors is 0.003 mag while for  $V > 12.7$  it is 0.03 mag (Figure 7, bottom panel). This is not due to increased measurement errors when the source fades, since the average errors in the range  $V < 12.7$  and  $V > 12.7$  are the same. The colors are constant, except for observations before MJD 9500, at the start of the campaign, and at MJD 9672, at the end, when the source was faint ( $\langle V \rangle = 12.87 \pm 0.11$  mag compared to  $\langle V \rangle = 12.55 \pm 0.19$  mag at the other times).

The 1994 June 3 (MJD 9506.9875) Lick spectrum of PKS 2155–304 is shown in Figure 8. The good data cover the wavelength range 4000 - 7500 Å. Excessive noise in the region redward of  $\sim 7600$  Å is an artifact of the high-amplitude interference fringes produced by the CCD; division by flatfields did not remove them completely, due to flexure of the spectrograph. Several weak features are visible in the optical region, but these are likely to be calibration errors; there appear to be no unambiguous absorption or emission lines to an equivalent width limit of  $\sim 1$  Å, and perhaps even 0.5 Å at most locations. Features typically observed in the spectra of these objects, if present, would be found at the locations marked (assuming  $z = 0.116$ ; Falomo, Pesce, & Treves 1993). A power law of index  $\alpha = -0.71 \pm 0.02$  (where  $F_\nu \propto \nu^\alpha$ ) provides a good fit to the spectrum. This is identical to the power-law index derived by Courvoisier et al. (1995) from Lick spectra of PKS 2155–304 obtained on 1991 October 31 and December 14.

As a further check of the continuum shape, we converted simultaneous magnitudes (mostly *UBVRI*, covering the range  $\sim 3600 - 9000$  Å) to fluxes using zero points from Bessell (1979). We then fit the continuum with a power law (as above) to get individual spectral slopes, and find an average  $\langle \alpha_{UBVRI} \rangle = -0.76 \pm 0.03$  (Figure 9, top panel). This is consistent with what we found from the Lick spectrum presented here, and what was found in previous studies (Smith & Sitko 1991; Smith et al. 1992; Courvoisier et al. 1995; Paltani et al. 1996). The spectra are slightly steeper during the period when  $V > 12.7$  (Figure 9, bottom panel).

### 3.2.3. *Polarization*

As with the 1991 November multiwavelength monitoring campaign (Smith et al. 1992), the optical polarization exhibited strong variability during 1994 May. The degree of linear polarization ( $P$ ) ranged from  $\sim 3\%$  to  $\sim 14\%$  (Table 8 and Figure 10, top panel) and the polarization position angle ( $\theta$ ) varied from  $\sim 100^\circ$  to  $\sim 150^\circ$  (Figure 10, bottom panel). Indeed, a change in  $\theta$  of nearly  $25^\circ$  was observed between May 15 and May 17 (MJD 9487.96 and 9489.95).

Broad-band *UBVRI* polarimetry acquired on May 19-21 (MJD 9491.96-9493.94) shows the development of strong wavelength-dependent polarization. Since only  $V$ -band measurements were made prior to May 19 (MJD 9492), it is impossible to know how  $P$  and/or  $\theta$  changed with wavelength during this period. However, it is apparent that any wavelength dependence was weak on May 19 ( $P_U/P_I = 1.03 \pm 0.19$ ), while on May 20 (MJD 9493)  $P$  clearly increases toward the blue ( $P_U/P_I = 1.15 \pm 0.08$ ). Strong wavelength dependence is observed on the following night, with  $P_U/P_I = 1.31 \pm 0.04$ . Though the

position angle exhibits no trend, the dependence on wavelength of  $P$  is among the strongest ever observed for PKS 2155–304, and we note that on May 21 (MJD 9493.9) the  $U$  polarization (14.3%) is the highest optical polarization reported for this object (cf. Smith et al. 1992). The increases in polarization after May 15 and 19 (MJD 9487.96 and 9491.96) correspond to the two ultraviolet flaring events (Urry et al. 1996).

Figure 11 shows the polarized  $V$ -band flux as a function of the  $V$ -band flux, ordered chronologically. Except for points 6-8, the optical photometry and polarization were not strictly simultaneous; there is a difference of about seven hours between measurements for points 1-4 and one day for point 5. There are no definite trends, and, in fact, PKS 2155–304 becomes both brighter and fainter as the polarization increases. The ultraviolet flaring events occur after observations 3 and 6.

Polarization observations later in the year (Table 9) show a general decrease from about 10% in July to around 5% in October (for the  $B$  and  $V$  bands, at least). At the same time, the object was brightening at all optical bands. It is interesting to note that the polarization position angle shows no preferred trend with percent polarization; for these observations it decreases with decreasing polarization, while in May it both increased and decreased with increasing polarization.

However, the observed position angles of PKS 2155–304 have been mostly confined between about 90° and 150° (Smith et al. 1992; Allen et al. 1993; Jannuzi, Smith, & Elston 1993). This has also been the case for the data collected during the period covered in this paper (Tables 8 and 9, Figure 10 bottom panel), in contrast to, for example, BL Lac itself (Moore et al. 1982). The preferred polarization orientation for PKS 2155–304 may indicate that the line of sight to PKS 2155–304 is not as close to the symmetry axis as may be the case for BL Lac. These two examples also reflect the general difference between X-ray-selected BL Lac objects (like PKS 2155–304) and radio-selected BL Lacs (like BL Lac itself) in that X-ray selected objects have preferred position angles more often than radio selected ones (Jannuzi, Smith, & Elston 1994).

The USP CCD imaging polarimetry also allowed measurements of the foreground stars in the field of PKS 2155–304. From  $V$  filter images taken on July 2, we selected seven stars. A weighted average of the measured Q/I and U/I Stokes parameters yielded  $P = (0.31 \pm 0.03)\%$  at 114°.5. In our fields, star No. 5 of Hamuy & Maza (1989) shows  $P = (0.27 \pm 0.04)\%$  at 121°.1, in excellent agreement with the field average. This corroborates earlier findings (Courvoisier et al. 1995) that the interstellar polarization towards PKS 2155–304 is negligible.

#### 4. Conclusions

In 1994 May the bright BL Lac object PKS 2155–304 was the subject of a large multiwavelength campaign. In this paper, we presented the ground-based radio, near-infrared, and optical results of the campaign, along with additional observations made throughout the year to 1994 November.

The 8.4, 15, and 22.5 GHz data seem to vary together over the observation period. There is possibly a lag of several days between the 8.4 and 15 GHz data and those at 22.5 GHz. When compared to the optical data obtained over the same period, there is no direct correlation, although the 4.8 GHz data from the first 10 days of observations may correlate with the optical data, with no measured lags. Any correlation between the radio and optical could be spurious, however, since there are variations on timescales of several days in both wavebands and many large gaps in coverage.

The millimeter data are essentially invariant, although variations of  $\sim 30\%$  are possible within the large errors. The near-infrared points exhibit a monotonic increase in brightness over their short observation period. Both of these data sets show variations comparable to what is seen in the optical and radio and there are no apparent correlations. The light curves in the optical bandpasses vary together and show similar short- and long-scale characteristics throughout the observation period. The fastest variations, of  $0.01 \text{ mag min}^{-1}$ , make PKS 2155–304 the most optically rapidly variable BL Lac observed to date and are similar to timescales observed in the UV (Pian et al. 1996). More typically, variations are  $\sim 0.01 \text{ mag hour}^{-1}$  or several tenths of a magnitude over days, which is what is seen for other blazars (e.g., Carini & Miller 1992). With a large number of assumptions, we limit the mass of the central black hole to  $M_{\text{var}} \lesssim 1.5 \times 10^9 (\frac{\delta}{10}) M_{\odot}$ ; this is consistent with the mass determined from UV and X-ray constraints, and considerably less than what was determined previously in the optical.

Smith et al. (1992) and Courvoisier et al. (1995) found the source to have constant color. Trends in  $B - V$  color have been noted before in the sense of bluer  $B - V$  as the source fades (Miller & McAlister 1983; Carini & Miller 1992), but during the present campaign the opposite occurred, with slightly redder colors as the source faded, similar to what was found by Treves et al. (1989) and Smith & Sitko (1991). The effect is small, however. The optical fluxes tracked each other well, indicating that intensive, multi-band optical monitoring is not necessary for such campaigns. Instead, the object can be observed several times per night in all bands, but intensively in just two or three.

Polarimetry measurements showed marked color dependence of the polarization (higher polarization toward the blue), in fact the strongest such dependence ever observed for

PKS 2155–304. The object was also seen to have the highest optical polarization observed ( $U = 14.3\%$ ), although in the range typical for X-ray selected BL Lacs (Jannuzi et al. 1994). Also typical for X-ray selected objects is the preferred position angle of the polarization we observed for PKS 2155–304.

J.E.P., E.P., and C.M.U. would like to acknowledge support from NASA grants NAG5-1918, NAG5-1034, and NAG5-2499. H.D.A. and M.F.A. acknowledge support from NSF grant AST-9421979, A.V.F. from NSF grant AST-8957063, E.J.H. from NASA Grant NGT-51152, R.I.K. and C.P. from NASA LTSA NAGW-2120, and P.S.S. from NASA Grant NAG5-1630. M.D.J. would like to thank the BYU Department of Physics and Astronomy for continued support of his research. A.M.M. and C.V.R. received support from the São Paulo state funding agency FAPESP through grant No. 94/0033-3. The University of Michigan Radio Astronomy Observatory is supported by the National Science Foundation and by funds from the University of Michigan. Sergio Ortolani is thanked for providing data. Some observations were obtained in the service observing mode from the JKT on La Palma; the help of Vik Dhillon, Derek Jones, Reynier Peletier, and Keith Tritton and the two service observers, Phil Rudd and Emilios Harlaftis, is greatly appreciated. The SAAO CCD data (D. Buckley) were obtained using a focal reducer provided by Dr. M. Shara (STScI). This research made use of the NASA/IPAC Extragalactic Database (NED), operated by the Jet Propulsion Laboratory, Caltech, under contract with NASA, and of NASA’s Astrophysics Data System Abstract Service (ADS).

## REFERENCES

Allen, R. G., Smith, P. S., Angel, J. R. P., Miller, B. W., Anderson, S. F., & Margon, B. 1993, *ApJ*, 403, 610

Aller, H. D., Aller, M. F., Latimer, G. E., & Hodge, P. E. 1985, *ApJS*, 59, 513

Baars, J. M. W., Genzel, R., Pauliny-Toth, I. I. K., & Witzel, A. 1977, *A&A*, 61, 99

Bessell, M. S. 1979, *PASP*, 91, 589

Blandford, R. D., & Rees, M. J. 1978, in *The Pittsburgh Conference on BL Lacs*, ed. A. M. Wolfe (Pittsburgh: The University of Pittsburgh Press), p. 328

Booth, R. S., Delgado, G., Hagstrom, M., Johansson, L. E. B., & Murphy, D. C. 1989, *A&A*, 216, 315

Bregman, J. N., & Hufnagel, B. 1989, in *BL Lac Objects*, eds. L. Maraschi, T. Maccacaro, & M.-H. Ulrich (Berlin: Springer-Verlag) p. 150

Brinkmann, W., et al. 1994, A&A, 288, 433

Carini, M. T., & Miller, H. R. 1992, ApJ, 385, 146

Carini, M. T., Miller, H. R., & Goodrich, B. D. 1990, AJ, 100, 347

Carini, M. T., Miller, H. R., Noble, J. C., & Goodrich, B. D. 1992, AJ, 104, 15

Carter, B. S. 1990, MNRAS, 242, 1

Courvoisier, T. J.-L., et al. 1995, ApJ, 438, 108

Edelson, R. A., et al. 1995, ApJ, 438, 120

Falomo, R., Pesce, J. E., & Treves, A. 1993, ApJ, 411, L63

Frater, R. H., Brooks, J. W., & Whiteoak, J. B., 1992, JEEEA, 12, No. 2, 103

Fruscione, A., Bowyer, S., Königl, A., & Kahn, S. 1994, ApJ, 422, L55

Ghisellini, G., Maraschi, L., & Treves, A. 1985, A&A, 146, 204

Grandi, P., et al. 1996, ApJ, 459, 73

Hamuy, M., & Maza, J. 1989, AJ, 97, 720

Hughes, P. A., Aller, H. D., & Aller, M. F. 1989, ApJ, 341, 68

Jannuzzi, B. T., Smith, P. S., & Elston, R. 1993, ApJS, 85, 265

Jannuzzi, B. T., Smith, P. S., & Elston, R. 1994, ApJ, 428, 130

Kii, T., et al. 1996, in preparation

Königl, A. 1989, in BL Lac Objects, eds. L. Maraschi, T. Maccacaro, & M.-H. Ulrich (Berlin: Springer-Verlag) p. 321

Magalhães, A. M., Rodrigues, C. V., Margoniner, V. E., Pereyra, A., & Heathcote, S. 1996, in Polarimetry of the Interstellar Medium, eds. D. C. B. Whittet & W. Roberge (San Francisco: ASP), p. 118

Marscher, A. P., & Gear, W. K. 1985, ApJ, 298, 114

Marshall, H. L., Carone, T. E., & Fruscione, A. 1993, ApJ, 414, L53

Marshall, H. L., et al. 1996, in preparation

Massey, P., Strobel, K., Barnes, J. V., & Anderson, E. 1988, ApJ, 328, 315

Miller, H. R., Carini, M. T., & Goodrich, B. D. 1989, Nature, 337, 627

Miller, H. R., & McAlister, H. A. 1983, ApJ, 272, 26

Miller, J. S., & Stone, R. P. S. 1993, Lick Obs. Tech. Rep., No. 66

Moore, R. L., et al. 1982, ApJ, 260, 415

Morini, M., et al. 1986, *ApJ*, 306, L71

Oke, J. B., & Gunn, J. E. 1983, *ApJ*, 266, 713

Padovani, P., & Giommi, P. 1995, *ApJ*, 444, 567

Paltani, S., Courvoisier, T.J.-L., Bratschi, P., & Blecha, A. 1996, in *Blazar Variability*, eds. H. R. Miller & J. Webb (San Francisco: ASP), in press

Pian, E., et al. 1996, *ApJ*, submitted

Pica, A. J., Smith, A. G., Webb, J. R., Leacock, R. J., Clements, S., & Gombola, P. P. 1988, *AJ*, 96, 1215

Rabbette, M., McBreen, B., Steel, S., & Smith, N. 1996, *A&A*, 310, 1

Smith, P. S., Hall, P. B., Allen, R. G., Sitko, M. L. 1992, *ApJ*, 400, 115

Smith, P. S., Jannuzi, B. T., & Elston, R. 1991, *ApJS*, 77, 67

Smith, P. S., & Sitko, M. L. 1991, *ApJ*, 383, 580

Treves, A., et al. 1989, *ApJ*, 341, 733

Urry, C. M., et al. 1993, *ApJ*, 411, 614

Urry, C. M., et al. 1996, *ApJ*, submitted

Vestrand, W. T., Stacy, J. C., & Sreekumar, P. 1995, *ApJ*, 454, L93

Wagner, S. J., et al. 1996, *AJ*, 111, 2187

Wagner, S. J., & Witzel, A. 1995, *ARA&A*, 33, 163

**Table 1:** VLA Radio Data <sup>a</sup>

Date Observed	JD (-2,440,000)	Flux (mJy) <sup>b</sup>				
		1.5 GHz	5.0 GHz	8.4 GHz	15.0 GHz	22.5 GHz
1994 May 14	9487.04	...	...	465±1	499±1	488±3
May 15	9488.13	419±1	509±1	451±1	504±1	476±2
May 16	9489.08	...	...	465±1	506±1	481±2
May 17	9490.08	...	...	463±1	502±1	547±2
May 18	9491.07	...	...	466±1	500±1	527±2
May 21	9494.10	365±1	515±1	488±1	523±1	556±2
May 22	9495.06	...	...	498±1	542±1	536±2
May 23	9496.09	...	...	508±1	534±1	524±3
May 24	9497.03	...	...	509±1	556±1	524±2
May 26	9499.05	...	...	481±1	549±2	632±3
May 28	9501.05	395±1	537±1	486±2	545±1	517±3
Jun 01	9505.04	392±1	514±1	491±1	505±1	473±2

<sup>a</sup>VLA data from R. I. Kollgaard and C. Palma.

<sup>b</sup>Errors shown are the internal errors. Total uncertainties are ∼10%, as in Figure 1.

**Table 2:** UMRAO Radio Data <sup>a</sup>

Date Observed	JD (-2,440,000)	Flux (mJy) <sup>b</sup>		
		4.8 GHz	8.0 GHz	14.5 GHz
1994 Apr 29	9471.9708	470	...	...
May 02	9475.0574	...	...	450
May 03	9475.9784	...	...	420
May 04	9477.0253	...	490	...
May 05	9478.0535	...	...	430
May 06	9478.9718	...	...	440
May 10	9482.9608	380	...	...
May 19	9491.9450	...	420	...
May 20	9493.0255	...	...	520
May 27	9499.9081	490	...	...
Jul 31	9564.8854	...	380	...
Sep 15	9610.6574	...	...	510
Sep 17	9612.7281	...	720	...
Sep 21	9616.6107	540	...	...
Dec 04	9690.5060	...	520	...

<sup>a</sup>Data from the University of Michigan Radio Astronomy Observatory (UMRAO) courtesy of M. and H. Aller.

<sup>b</sup>Typical uncertainties on individual measurements are 40, 80, and 20 mJy at 4.8, 8.0, and 14.5 GHz, respectively.

**Table 3:** ATCA Centimeter Radio Data <sup>a</sup>

Date Observed	JD (-2,440,000)	Flux (mJy)			
		1.380 GHz (20 cm)	2.378 GHz (13 cm)	4.800 GHz (6 cm)	8.640 GHz (3 cm)
1994 May 04	9477.1708	378.1±48.9	383.1±26.3	...	...
May 04	9477.2007	...	...	404.9±21.7	336.5±19.9
May 04	9477.2236	377.2±44.8	380.0±24.7	...	...
May 04	9477.2576	...	...	392.4±21.8	326.5±18.7
May 04	9477.2806	369.2±48.0	374.1±23.4	...	...
May 04	9477.3160	...	...	394.2±20.5	328.7±17.9
May 04	9477.3368	369.3±86.6	376.0±22.8	...	...
May 04	9477.3931	...	...	401.2±20.7	331.5±18.3
May 04	9477.4063	357.8±33.2	377.7±24.1	...	...
May 04	9477.4236	...	...	400.8±21.1	330.0±18.2
May 04	9477.4465	373.4±82.2	384.1±22.9	...	...
May 04	9477.4688	...	...	401.7±21.8	332.6±18.5
May 04	9477.4917	376.2±64.1	386.2±23.6	...	...
May 05	9477.5271	368.0±47.8	390.0±24.7	...	...
May 05	9477.5493	...	...	406.8±22.1	332.1±20.0
May 05	9477.5722	370.9±47.4	392.5±26.5	...	...
May 05	9477.5951	...	...	413.3±24.3	337.7±21.8
May 05	9477.6097	377.9±51.2	392.7±29.7	...	...
May 19	9492.1972	...	...	417.5±30.2	406.2±27.6
May 19	9492.1979	395.1±35.0	406.9±32.8	...	...
May 19	9492.2764	...	...	412.6±27.9	399.4±26.9
May 19	9492.2778	377.0±37.7	400.4±31.6	...	...
May 20	9492.5583	...	...	422.4±33.4	409.5±34.0

**Table 3:** *continued.*

Date Observed	JD (-2,440,000)	Flux (mJy)			
		1.380 GHz (20 cm)	2.378 GHz (13 cm)	4.800 GHz (6 cm)	8.640 GHz (3 cm)
1994 May 20	9492.5597	378.1±40.4	405.2±40.0	...	...
May 20	9493.1368	...	...	434.3±30.0	414.5±33.2
May 20	9493.1375	392.7±39.0	417.0±35.2	...	...
May 20	9493.1958	...	...	429.3±27.9	415.5±29.2
May 20	9493.1965	405.5±41.5	422.5±32.5	...	...
May 20	9493.2660	...	...	426.4±27.8	415.1±28.2
May 20	9493.2667	373.6±37.5	412.2±32.3	...	...
May 20	9493.3708	...	...	429.2±26.6	419.7±28.5
May 20	9493.3715	360.8±32.1	404.1±32.0	...	...
May 20	9493.4583	...	...	431.0±29.6	427.8±29.5
May 20	9493.4597	366.2±40.1	404.8±33.8	...	...
May 21	9494.1958	...	...	422.9±28.2	421.8±28.8
May 21	9494.1965	366.3±40.4	392.1±33.1	...	...
May 21	9494.2708	...	...	416.0±27.0	416.3±28.4
May 21	9494.2722	361.1±34.6	390.7±30.6	...	...
May 22	9494.5611	...	...	427.3±34.9	421.5±35.7
May 22	9494.5618	383.1±43.1	395.0±43.3	...	...
May 22	9495.1243	...	...	429.4±31.0	434.7±34.0
May 22	9495.1250	369.0±46.6	384.2±36.4	...	...
May 22	9495.1826	...	...	423.3±28.8	433.8±29.7
May 22	9495.1840	367.7±39.5	387.3±34.8	...	...
May 22	9495.2528	...	...	421.2±28.3	428.1±30.2
May 22	9495.2542	367.1±32.0	381.9±32.5	...	...

**Table 3:** *continued.*

Date Observed	JD (-2,440,000)	Flux (mJy)			
		1.380 GHz (20 cm)	2.378 GHz (13 cm)	4.800 GHz (6 cm)	8.640 GHz (3 cm)
1994 Aug 30	9594.9340	474.9±35.0	467.8±32.6	...	...
Aug 30	9594.9354	...	...	482.2±30.9	479.7±35.9
Aug 30	9595.0035	455.3±32.1	463.8±32.7	...	...
Aug 30	9595.0049	...	...	478.1±33.3	477.1±48.7
Aug 30	9595.0889	460.0±32.8	461.7±32.9	...	...
Aug 30	9595.0903	...	...	473.9±34.2	465.4±45.3
Aug 30	9595.1785	480.7±36.2	466.6±34.1	...	...
Aug 30	9595.1799	...	...	476.2±29.6	472.2±34.9
Aug 30	9595.2653	493.8±37.6	474.7±36.1	...	...
Aug 30	9595.2674	...	...	491.4±30.6	484.8±32.3
Aug 31	9595.8764	508.6±36.8	486.2±33.0	...	...
Aug 31	9595.8778	...	...	486.3±30.1	484.8±30.0
Aug 31	9595.9813	502.8±34.7	475.2±31.1	...	...
Aug 31	9595.9826	...	...	476.2±26.0	471.5±27.0
Aug 31	9596.0639	496.2±33.5	476.9±32.1	...	...
Aug 31	9596.0653	...	...	481.5±25.9	475.9±27.8
Aug 31	9596.1597	497.4±32.5	477.9±32.2	...	...
Aug 31	9596.1604	...	...	483.2±28.0	479.8±28.3
Aug 31	9596.2556	503.0±43.3	476.5±35.5	...	...
Aug 31	9596.2569	...	...	487.7±30.2	481.2±31.5

<sup>a</sup>Data from L. Kedziora-Chudczer.

**Table 4:** SEST Millimeter Data

Date Observed	JD (-2,440,000)	Flux (mJy)		
		90 GHz <sup>a</sup>	94 GHz <sup>b</sup>	230 GHz <sup>a</sup>
1994 Apr 24	9467.139	355±71	...	...
Apr 25	9468.122	348±41	...	...
Apr 25	9468.215	417±57	...	...
May 19	9492.094	...	367±78	...
May 21	9494.104	...	367±78	...
Jun 01	9504.778	430±81	...	...
Jun 25	9528.751	...	...	310±24
Jun 25	9528.788	...	...	330±25
Jun 26	9529.754	450±117	...	...

---

<sup>a</sup>Data from M. Tornikoski.

<sup>b</sup>Data from L.B.G. Knee.

**Table 5:** Optical/Near-IR Observers and Telescopes

Observer	Telescope	Filters	Code <sup>a</sup>
A. Barth	Lick 3m	...	...
D. Buckley	SAAO 1.9m	Johnson-Cousins ( $UBVR_c I_c$ )	DB
E. Covino	ESO 1m	Johnson-Cousins ( $UBVR_c I_c$ )	EC
A. Filippenko	Lick 3m	...	...
E. Hooper	Steward 90in	Johnson-Cousins ( $BVR_c I_c$ )	EH
M. Joner	CTIO 0.9m	Johnson-Cousins ( $BVR_c I_c$ )	MJ
D. Kilkenny	SAAO 0.5m	Johnson-Cousins ( $UBVR_c I_c$ )	DK
M. Kunkel	ESO 1m	ESO ( $JHKL$ )	MK
A. Layden	KPNO 0.9m	Johnson-Cousins ( $BVR_c I_c$ )	ALKP
A. Layden	CTIO 0.9m	Johnson-Cousins ( $BVR_c I_c$ )	ALCT
M. Magalhães	Univ. of São Paulo 0.61m	Johnson ( $BV$ )	MM
F. Marang	SAAO 0.5m	Johnson-Cousins ( $UBVR_c I_c$ )	FM
S. Ortolani	ESO 1.5m Danish	Johnson ( $BV$ )	SO
J. Pesce	La Palma JKT (Service)	Johnson-Cousins ( $BVR_c I_c$ )	JEP/JKT
C. Rodrigues	Univ. of São Paulo 0.61m	Johnson ( $BV$ )	CR
A. Schutte	SAAO 1.9m	SAAO ( $JHKL$ )	AS
P. Smith	Steward 1.5m	Johnson-Cousins ( $UBVR_c I_c$ )	PSS
P. Smith	U. of Minn. 1.5m	Johnson-Cousins ( $UBVR_c I_c$ )	...
J. van der Walt	SAAO 1.9m	SAAO ( $JHKL$ )	JvdW
F. van Wyk	SAAO 0.5m	Johnson-Cousins ( $UBVR_c I_c$ )	FvW
P. Whitelock	SAAO 1.9m	SAAO ( $JHKL$ )	PW
S. Wolk	CTIO 0.9m	Johnson-Cousins ( $BVR_c I_c$ )	SW

<sup>a</sup>Observer codes are used in Tables 6 and 7.

**Table 6:** Near-Infrared Data

Date Observed	JD (-2,440,000)	<i>J</i>	<i>H</i>	<i>K</i>	<i>L</i>	Observer <sup>a</sup>
1994 May 19	9491.68	11.51±0.03	10.82±0.03	10.18±0.03	9.14±0.05	PW
May 20	9492.66	11.47±0.03	10.78±0.03	10.13±0.03	9.06±0.05	PW
May 24	9496.68	11.36±0.03	10.6±0.03	9.98±0.03	8.95±0.05	PW
May 24	9496.95	11.51±0.02	10.74±0.01	9.99 ±0.02	9.85±0.6	MK <sup>b</sup>
May 25	9497.65	11.34±0.03	10.62±0.03	9.99±0.03	8.88±0.08	AS/JvdW
May 26	9498.66	11.30±0.03	10.59±0.03	9.93±0.03	8.88±0.08	AS/JvdW

<sup>a</sup>Observers are listed in Table 5.

<sup>b</sup>Magnitudes from MK were originally from the ESO standard system and have been converted to the SAAO system (see text).

**Table 7:** Optical Data

Date Observed	JD (-2,440,000)	<i>U</i> <sup>a</sup>	<i>B</i> <sup>a</sup>	<i>V</i> <sup>a</sup>	<i>R</i> <sup>a</sup>	<i>I</i> <sup>a</sup>	Observer <sup>b</sup>
1994 May 02	9474.9173	12.33	13.21	13.02	12.76	12.31	EC
May 04	9476.8737	12.59	13.29	12.98	12.67	12.26	EC
May 05	9477.8953	12.65	13.29	13.03	12.73	12.33	EC
May 08	9480.9778	...	...	...	12.83	...	EH
May 08	9480.9813	...	13.66	...	...	...	EH
May 08	9480.9826	...	13.67	...	...	...	EH
May 08	9480.9861	...	...	13.14	...	...	EH
May 08	9480.9882	...	...	...	...	12.42	EH
May 08	9480.9896	...	...	...	12.84	...	EH
May 11	9483.6832	13.17	...	...	...	...	DB
May 11	9483.6867	...	...	12.73	...	...	DB
May 11	9483.6876	...	...	...	12.46	...	DB
May 11	9483.6884	...	...	...	...	12.46	DB
May 12	9484.6826	13.13	...	...	...	...	DB
May 12	9484.6857	...	...	13.01	...	...	DB
May 12	9484.6870	...	...	...	12.66	...	DB
May 13	9485.6762	12.95	...	...	...	...	DB
May 13	9485.6786	...	13.28	...	...	...	DB
May 13	9485.6794	...	...	12.85	...	...	DB
May 13	9485.6802	...	...	...	12.67	...	DB
May 13	9485.6810	...	...	...	...	12.32	DB
May 14	9486.6609	13.12	...	...	...	...	DB
May 14	9486.6638	...	13.35	...	...	...	DB
May 14	9486.6645	...	...	12.91	...	...	DB

**Table 7:** - *continued.*

Date Observed	JD (-2,440,000)	<i>U</i> <sup>a</sup>	<i>B</i> <sup>a</sup>	<i>V</i> <sup>a</sup>	<i>R</i> <sup>a</sup>	<i>I</i> <sup>a</sup>	Observer <sup>b</sup>
1994 May 14	9486.6652	...	...	...	12.66	...	DB
May 14	9486.6659	...	...	...	...	12.34	DB
May 14	9486.6726	...	13.22	...	...	...	DB
May 14	9486.6734	...	...	12.88	...	...	DB
May 14	9486.6742	...	...	...	12.58	...	DB
May 14	9486.6753	...	...	...	...	12.16	DB
May 15	9487.6542	...	13.21	...	...	...	DB
May 15	9487.6575	...	...	12.79	...	...	DB
May 16	9488.6347	...	13.15	...	...	...	DB
May 16	9488.6382	...	...	12.81	...	...	DB
May 16	9488.6595	...	...	...	12.54	...	DB
May 16	9488.6623	...	...	...	...	12.11	DB
May 18	*9490.9888	...	...	...	12.55	...	ALKP
May 18	*9490.9919	...	...	12.87	...	...	ALKP
May 19	*9491.9618	...	...	12.97	...	...	PSS
May 19	*9491.9846	...	...	...	12.64	...	ALKP
May 19	*9491.9869	...	...	12.96	...	...	ALKP
May 20	*9492.9271	...	13.20	12.81	...	...	SO
May 20	*9492.9597	...	...	12.82	...	...	PSS
May 20	*9492.9817	...	...	...	12.47	...	ALKP
May 21	*9493.9563	...	...	12.69	...	...	PSS
May 22	*9494.7889	...	13.20	...	...	...	MJ
May 22	*9494.7917	...	...	12.86	...	...	MJ

**Table 7:** - *continued.*

Date Observed	JD (-2,440,000)	<i>U</i> <sup>a</sup>	<i>B</i> <sup>a</sup>	<i>V</i> <sup>a</sup>	<i>R</i> <sup>a</sup>	<i>I</i> <sup>a</sup>	Observer <sup>b</sup>
1994 May 22	*9494.7937	...	...	...	12.62	...	MJ
May 22	*9494.7954	...	...	...	...	12.18	MJ
May 22	*9494.8664	...	...	12.90	...	...	MJ
May 22	*9494.8693	...	13.24	...	...	...	MJ
May 25	*9497.8342	...	...	...	...	12.04	MJ
May 25	*9497.8354	...	...	...	...	12.05	MJ
May 25	*9497.8373	...	...	...	12.46	...	MJ
May 25	*9497.8385	...	...	...	12.47	...	MJ
May 25	*9497.8402	...	...	12.76	...	...	MJ
May 25	*9497.8418	...	...	12.81	...	...	MJ
May 25	*9497.8454	...	13.06	...	...	...	MJ
May 25	*9497.8491	...	13.06	...	...	...	MJ
May 25	*9497.8528	...	13.06	...	...	...	MJ
May 26	*9498.8535	...	...	12.73	...	...	MM/CR
May 26	*9498.8603	...	13.23	...	...	...	MM/CR
May 26	*9498.8728	...	13.08	...	...	...	MJ
May 26	*9498.8750	...	13.08	...	...	...	MJ
May 26	*9498.8776	...	...	12.76	...	...	MJ
May 26	*9498.8789	...	...	12.76	...	...	MJ
May 26	*9498.8805	...	...	...	12.45	...	MJ
May 26	*9498.8814	...	...	...	12.44	...	MJ
May 26	*9498.8832	...	...	...	...	12.04	MJ
May 26	*9498.8841	...	...	...	...	12.02	MJ

**Table 7:** - *continued.*

Date Observed	JD (-2,440,000)	<i>U</i> <sup>a</sup>	<i>B</i> <sup>a</sup>	<i>V</i> <sup>a</sup>	<i>R</i> <sup>a</sup>	<i>I</i> <sup>a</sup>	Observer <sup>b</sup>
1994 May 27	9499.9454	...	...	12.86	...	...	SW
May 27	9499.9478	...	...	...	12.50	...	SW
May 27	9499.9495	...	...	...	...	12.14	SW
May 31	9503.9392	...	...	12.74	...	...	SW
May 31	9503.9413	...	...	...	12.41	...	SW
Jun 03	9506.9386	...	12.85	...	...	...	SW
Jun 03	9506.9411	...	...	12.65	...	...	SW
Jun 03	9506.9459	...	...	...	...	11.92	SW
Jun 04	9507.9301	...	12.94	...	...	...	SW
Jun 04	9507.9325	...	...	12.72	...	...	SW
Jun 12	9515.5978	12.15	12.85	12.55	12.25	11.86	DK/FM/FvW
Jun 14	9517.6211	12.24	12.94	12.63	12.32	11.92	DK/FM/FvW
Jun 15	9518.6302	12.32	13.01	12.68	12.38	11.98	DK/FM/FvW
Jun 16	9519.6477	12.38	13.07	12.74	12.44	12.08	DK/FM/FvW
Jun 22	9525.6015	12.45	13.11	12.88	12.58	12.17	DK/FM/FvW
Jun 26	9529.9427	...	...	...	...	12.15	ALCT
Jun 26	9529.9438	...	...	12.86	...	...	ALCT
Jun 26	9529.9452	...	13.10	...	...	...	ALCT
Jun 27	9530.8505	...	13.06	...	...	...	ALCT
Jun 27	9530.8538	...	...	12.80	...	...	ALCT
Jun 27	9530.8554	...	...	...	...	12.04	ALCT
Jun 27	9530.8616	...	...	...	...	12.10	ALCT
Jul 01	9534.6218	12.31	13.02	12.71	12.42	12.03	DK/FM/FvW
Jul 02	9535.6036	12.36	13.05	12.73	12.43	12.03	DK/FM/FvW

**Table 7:** - *continued.*

Date Observed	JD (-2,440,000)	<i>U</i> <sup>a</sup>	<i>B</i> <sup>a</sup>	<i>V</i> <sup>a</sup>	<i>R</i> <sup>a</sup>	<i>I</i> <sup>a</sup>	Observer <sup>b</sup>
1994 Jul 03	9536.6211	12.35	13.05	12.74	12.44	12.06	DK/FM/FvW
Jul 04	9537.5886	12.26	12.97	12.68	12.37	12.00	DK/FM/FvW
Jul 05	9538.5756	12.45	13.14	12.83	12.51	12.10	DK/FM/FvW
Jul 06	9539.5865	12.45	13.15	12.82	12.52	12.12	DK/FM/FvW
Jul 07	9540.5710	12.44	13.14	12.82	12.52	12.11	DK/FM/FvW
Jul 08	9541.5812	12.43	13.12	12.80	12.49	12.07	DK/FM/FvW
Jul 09	9542.6156	12.39	13.10	12.79	12.49	12.10	DK/FM/FvW
Jul 12	9545.5740	12.34	13.04	12.74	12.44	12.04	DK/FM/FvW
Jul 13	9546.5510	12.38	13.09	12.78	12.48	12.08	DK/FM/FvW
Jul 14	9547.5769	12.41	13.10	12.79	12.49	12.10	DK/FM/FvW
Jul 20	9553.6226	...	13.02	...	...	...	JEP/JKT
Jul 20	9553.6290	...	13.02	...	...	...	JEP/JKT
Jul 20	9553.6341	...	13.02	...	...	...	JEP/JKT
Jul 20	9553.6390	...	...	12.67	...	...	JEP/JKT
Jul 20	9553.6437	...	...	12.66	...	...	JEP/JKT
Jul 20	9553.6520	...	...	...	12.35	...	JEP/JKT
Jul 20	9553.6555	...	...	...	12.34	...	JEP/JKT
Jul 20	9553.6618	...	...	...	...	11.93	JEP/JKT
Jul 20	9553.6682	...	...	...	...	11.94	JEP/JKT
Jul 28	9561.5073	12.14	12.84	12.52	12.22	11.80	DK/FM/FvW
Jul 29	9562.5073	12.13	12.82	12.53	12.23	11.83	DK/FM/FvW
Jul 30	9563.5061	12.22	12.92	12.62	12.31	11.91	DK/FM/FvW
Aug 01	9566.4992	12.19	12.89	12.58	12.28	11.91	DK/FM/FvW
Aug 02	9566.5353	...	12.93	...	...	...	JEP/JKT

**Table 7:** - *continued.*

Date Observed	JD (-2,440,000)	<i>U</i> <sup>a</sup>	<i>B</i> <sup>a</sup>	<i>V</i> <sup>a</sup>	<i>R</i> <sup>a</sup>	<i>I</i> <sup>a</sup>	Observer <sup>b</sup>
1994 Aug 02	9566.5425	...	12.96	...	...	...	JEP/JKT
Aug 02	9566.5491	...	...	12.60	...	...	JEP/JKT
Aug 02	9566.5535	...	...	12.62	...	...	JEP/JKT
Aug 02	9566.5561	...	...	...	12.30	...	JEP/JKT
Aug 02	9566.5604	...	...	...	12.29	...	JEP/JKT
Aug 02	9566.5627	...	...	...	...	11.90	JEP/JKT
Aug 02	9566.5668	...	...	...	...	11.89	JEP/JKT
Aug 10	9575.4039	12.01	12.72	12.44	12.15	11.78	DK/FM/FvW
Aug 10	9575.4813	12.00	12.71	12.42	12.13	11.75	DK/FM/FvW
Aug 11	9576.4048	12.12	12.82	12.51	12.22	11.82	DK/FM/FvW
Aug 11	9576.4830	12.12	12.82	12.51	12.21	11.82	DK/FM/FvW
Aug 12	9576.5704	12.12	12.82	12.51	12.22	11.81	DK/FM/FvW
Aug 15	9580.4852	11.96	12.65	12.36	12.07	11.68	DK/FM/FvW
Aug 16	9580.5576	11.97	12.67	12.36	12.07	11.66	DK/FM/FvW
Aug 16	9581.4061	11.92	12.62	12.32	12.04	11.67	DK/FM/FvW
Aug 16	9581.4547	11.90	12.60	12.31	12.01	11.63	DK/FM/FvW
Aug 17	9581.5542	11.88	12.55	12.28	12.00	11.66	DK/FM/FvW
Aug 17	9582.3906	11.93	12.61	12.32	12.02	11.62	DK/FM/FvW
Aug 17	9582.4599	11.90	12.61	12.30	12.02	11.62	DK/FM/FvW
Aug 18	9582.5257	11.90	12.61	12.31	12.02	11.65	DK/FM/FvW
Aug 21	9586.3861	12.06	12.70	12.40	12.14	11.72	DK/FM/FvW
Aug 21	9586.4330	12.04	12.76	12.44	12.13	11.75	DK/FM/FvW
Aug 22	9586.5211	12.07	12.81	12.49	12.16	11.79	DK/FM/FvW
Aug 22	9587.3876	11.99	12.72	12.39	12.09	11.66	DK/FM/FvW

**Table 7:** - *continued.*

Date Observed	JD (-2,440,000)	<i>U</i> <sup>a</sup>	<i>B</i> <sup>a</sup>	<i>V</i> <sup>a</sup>	<i>R</i> <sup>a</sup>	<i>I</i> <sup>a</sup>	Observer <sup>b</sup>
1994 Aug 22	9587.4385	11.99	12.73	12.42	12.09	11.69	DK/FM/FvW
Aug 23	9587.5223	12.03	12.76	12.46	12.09	11.77	DK/FM/FvW
Aug 25	9590.4331	11.99	12.67	12.34	12.02	11.61	DK/FM/FvW
Aug 29	9594.4065	11.98	12.68	12.36	12.04	11.65	DK/FM/FvW
Sep 02	9597.5145	11.91	12.61	12.31	12.01	11.59	DK/FM/FvW
Sep 02	9598.4908	11.99	12.67	12.36	12.06	11.65	DK/FM/FvW
Sep 05	9601.4694	12.03	12.71	12.36	12.05	11.64	DK/FM/FvW
Sep 08	9604.3906	11.90	12.59	12.27	11.96	11.55	DK/FM/FvW
Sep 11	9607.3721	12.00	12.70	12.39	12.09	11.71	DK/FM/FvW
Sep 12	9608.3965	11.87	12.57	12.28	11.98	11.59	DK/FM/FvW
Nov 16	9672.6097	...	...	...	12.44	...	EH
Nov 16	9672.6167	...	13.24	...	...	...	EH
Nov 16	9672.6285	...	...	12.74	...	...	EH
Nov 16	9672.6403	...	...	...	...	12.01	EH

<sup>a</sup>For all passbands, uncertainties are typically 0.01 mag.

<sup>b</sup>Observers are listed in Table 5.

\*Simultaneous space-based data available on these dates.

**Table 8:** Two-Holer Polarization Data <sup>a</sup>

Date Observed	JD (-2,440,000)	Filter	P (%)	PA ( $^{\circ}$ )
1994 May 19	9491.95	<i>U</i>	5.53 $\pm$ 0.94	157.1 $\pm$ 4.8
	9492.95	<i>U</i>	8.84 $\pm$ 0.48	137.9 $\pm$ 1.6
	9493.95	<i>U</i>	14.25 $\pm$ 0.35	133.0 $\pm$ 0.7
May 19	9491.96	<i>B</i>	6.23 $\pm$ 0.37	151.1 $\pm$ 1.7
	9492.94	<i>B</i>	8.76 $\pm$ 0.35	136.4 $\pm$ 1.1
	9493.94	<i>B</i>	13.19 $\pm$ 0.30	131.8 $\pm$ 0.6
May 13	9485.97	<i>V</i>	7.57 $\pm$ 0.67	96.5 $\pm$ 2.5
	9486.96	<i>V</i>	7.52 $\pm$ 0.81	101.7 $\pm$ 3.1
	9487.96	<i>V</i>	2.88 $\pm$ 0.29	98.0 $\pm$ 2.9
	9488.96	<i>V</i>	4.99 $\pm$ 0.22	108.9 $\pm$ 1.3
	9489.95	<i>V</i>	6.54 $\pm$ 0.36	132.1 $\pm$ 1.6
	9491.96	<i>V</i>	5.92 $\pm$ 0.28	150.1 $\pm$ 1.3
	9492.96	<i>V</i>	8.02 $\pm$ 0.30	135.3 $\pm$ 1.1
	9493.95	<i>V</i>	12.31 $\pm$ 0.21	131.5 $\pm$ 0.5
	9491.95	<i>R</i>	5.68 $\pm$ 0.29	151.2 $\pm$ 1.4
May 20	9492.94	<i>R</i>	7.54 $\pm$ 0.33	134.9 $\pm$ 1.2
	9493.93	<i>R</i>	11.90 $\pm$ 0.21	132.0 $\pm$ 0.5
	9491.95	<i>I</i>	5.38 $\pm$ 0.30	150.8 $\pm$ 1.6
May 21	9492.95	<i>I</i>	7.70 $\pm$ 0.36	135.5 $\pm$ 1.3
	9493.94	<i>I</i>	10.89 $\pm$ 0.24	132.6 $\pm$ 0.6

<sup>a</sup>Observations by P. Smith with the Univ. of Minnesota 1.5m (1994 May 13-17) and the Steward Observatory 1.5m (1994 May 19-21) telescopes, both on Mt. Lemmon, Arizona.

**Table 9:** LNA and USP Polarization Data <sup>a</sup>

Date Observed	JD (-2,440,000)	Filter	P (%)	PA (°)
1994 Jul 05	9538.83	<i>B</i>	10.04±0.14	114.1±0.4
Oct 13	9638.53	<i>B</i>	5.16±0.06	96.8±0.3
Jul 02	9535.80	<i>V</i>	11.29±0.15	105.0±0.4
Jul 21	9554.83	<i>V</i>	8.12±0.15	94.7±0.5
Sep 01	9596.79	<i>V</i>	5.36±0.04	95.1±0.2
Oct 13	9638.57	<i>V</i>	5.36±0.07	95.5±0.4
Jul 02	9535.85	<i>R</i>	10.28±0.05	101.6±0.1
Jul 21	9554.79	<i>R</i>	7.33±0.10	94.1±0.4
Jul 05	9538.71	<i>I</i>	9.20±0.09	118.9±0.3
Jul 25	9558.70	<i>I</i>	7.38±0.07	101.4±0.3
Jul 03	9536.78	none	10.22±0.08	104.3±0.2

---

<sup>a</sup>Observations by A. Magalhães V. Margoniner, A. Pereyra, and C. Rodrigues with the LNA 1.60m and USP 0.61m telescopes.

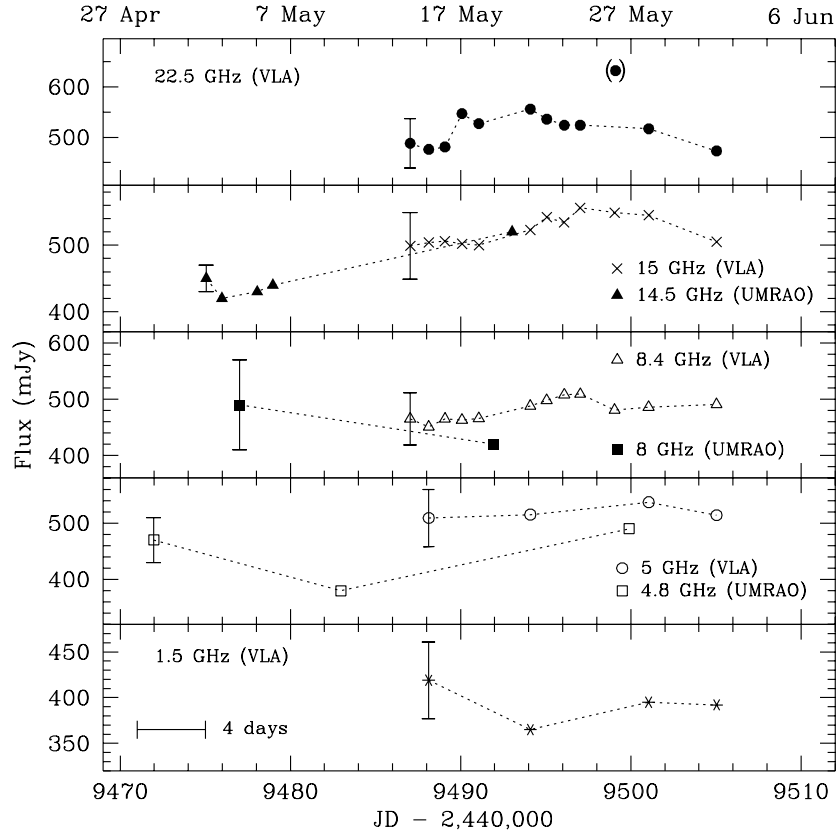


Fig. 1.— The radio light curves from 1994 April to June. The 22.5, 15, and 8.4 GHz data show a slight (10% - 20%) increase in flux and then a decrease by the same amount over the observation period. The 14.5 GHz data increase by the same amount, while the other bands are basically invariant. Uncertainties are shown on the first point of each light curve and are  $\pm 10\%$  for the VLA data and  $\pm 40, 80$ , and  $20$  mJy for the UMRAO 4.8, 8.0, and 14.5 GHz data, respectively. The large 22.5 GHz peak on May 26 (MJD 9499.05) is probably an artifact. The lines have been added to guide the eye only.

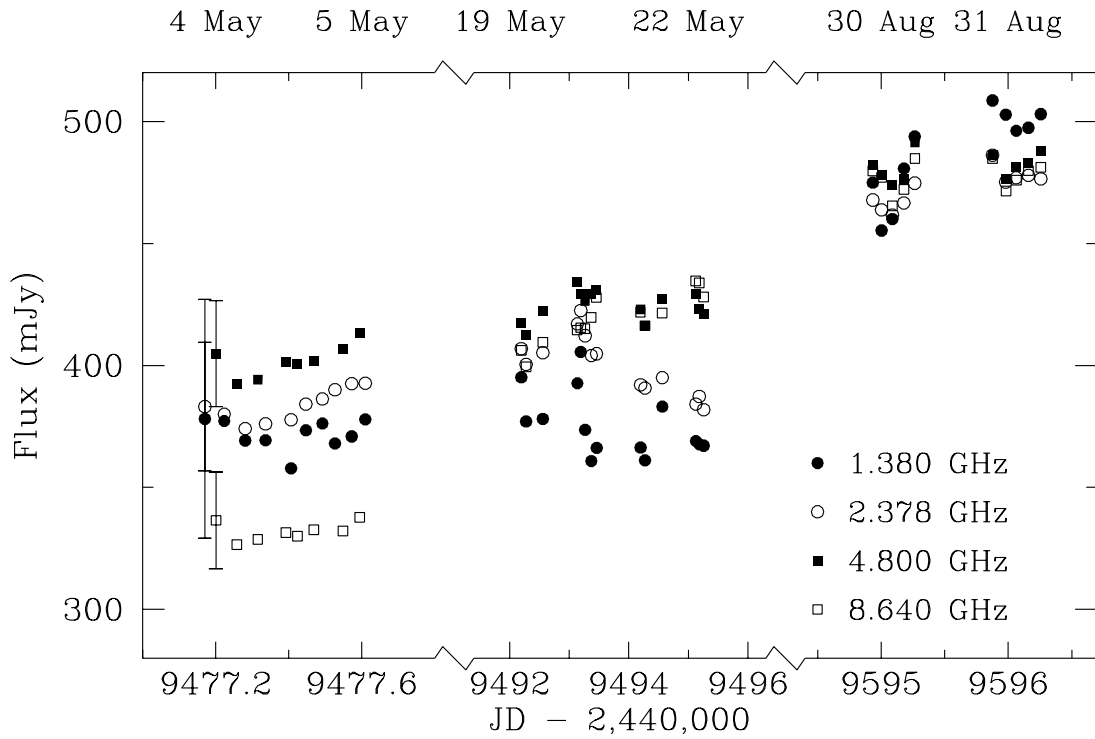


Fig. 2.— The centimeter light curves from ATCA. The source brightens slightly (20-40%) over the observation period (May - August) and there is a strong change in the spectral index between early and mid May and again between mid May and late August.

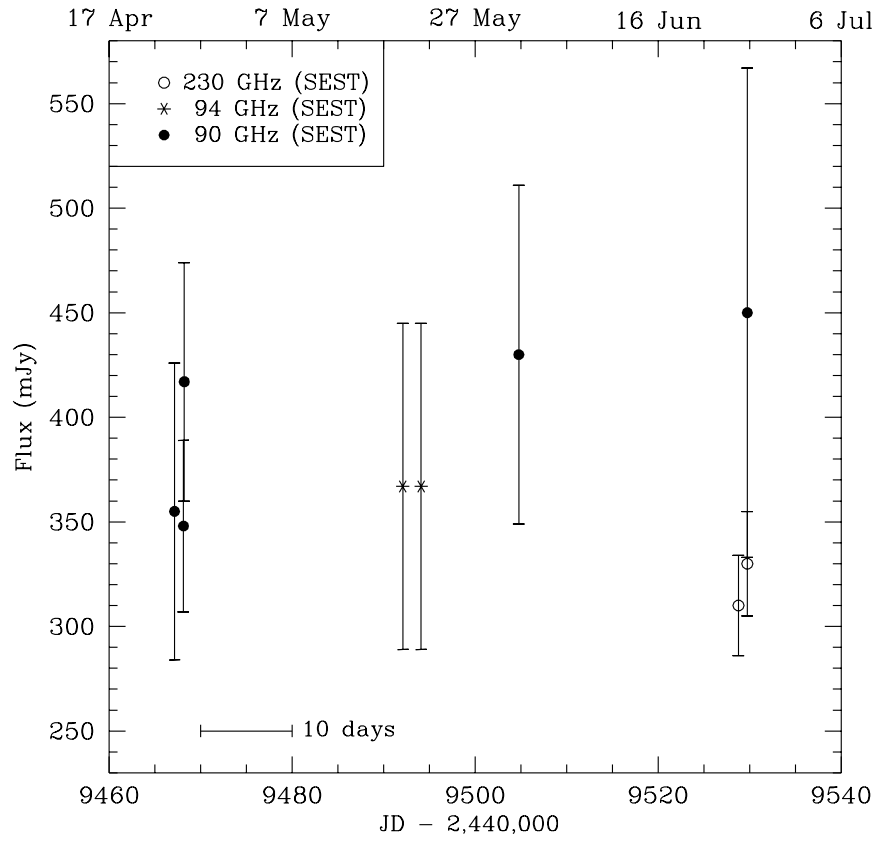


Fig. 3.— The millimeter light curves from SEST. No variations are obvious. A time scale bar is shown for comparison with the other figures.

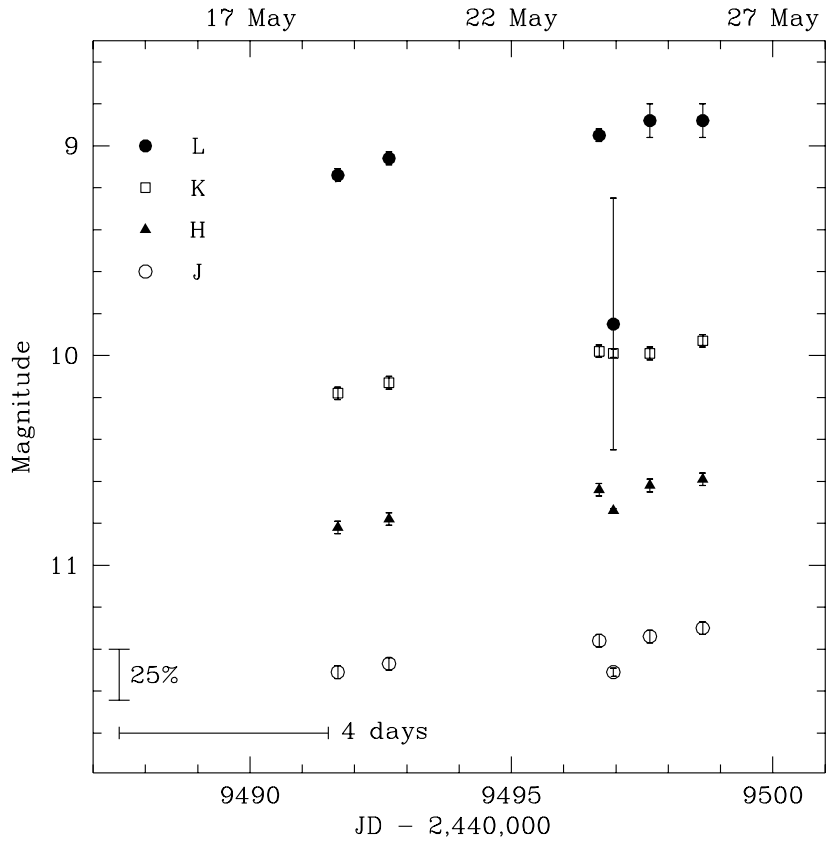


Fig. 4.— The near-infrared light curves from 1994 May. All bands increase by  $\sim 0.3$  mag over the period of observations. The  $L$  magnitude on MJD 9496.95 is probably spurious, whereas the dip seen in  $H$  and  $J$  on the same day may be real but instrumental effects cannot be ruled out. A time scale bar is shown for comparison with the other figures.

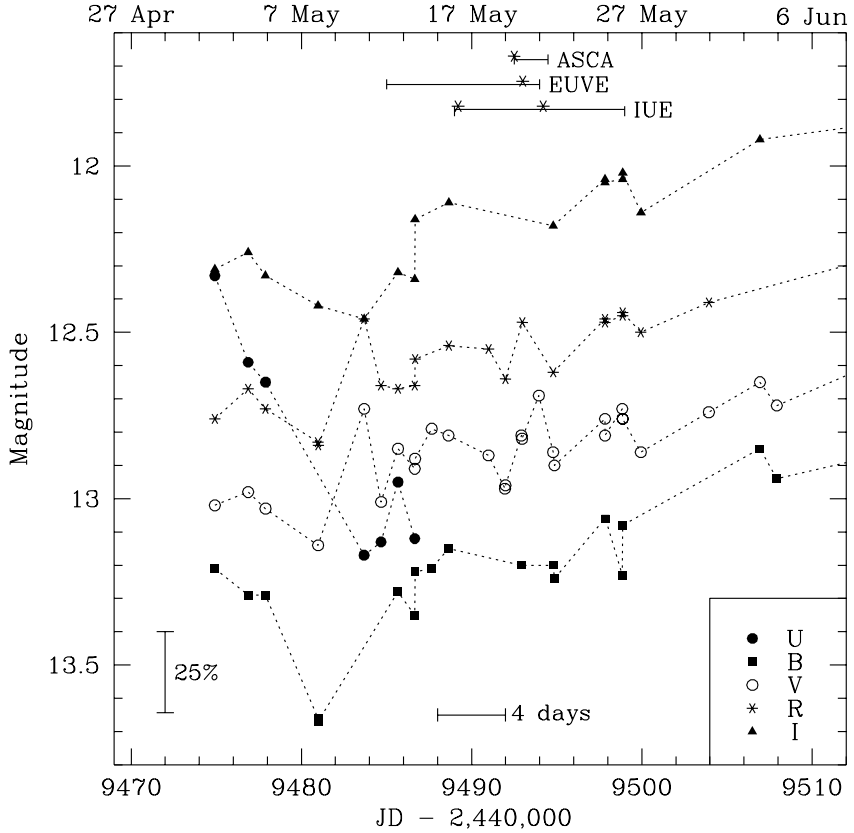


Fig. 5.— The optical light curves during the multiwavelength monitoring campaign, 1994 May. Where coverage is sufficient, it can be seen that all bands vary together. The  $V$ - and  $R$ -band fluxes show a feature between MJD 9492 and 9495 which corresponds to the UV flare. Note the  $I$ -band flux increase on  $\sim$ 13 May (MJD 9486). This corresponds to a variation of  $0.01 \text{ mag min}^{-1}$ . Uncertainties are the size of the points or smaller (they range from  $\lesssim 0.01$  to  $\sim 0.08$  mag, with 0.01 mag being typical). The durations of the *ASCA*, *EUVE*, and *IUE* experiments are shown at the top of the figure, and the midpoints of the flares are indicated with asterisks. A time scale bar is shown for comparison with the other figures. The lines have been added to guide the eye only.

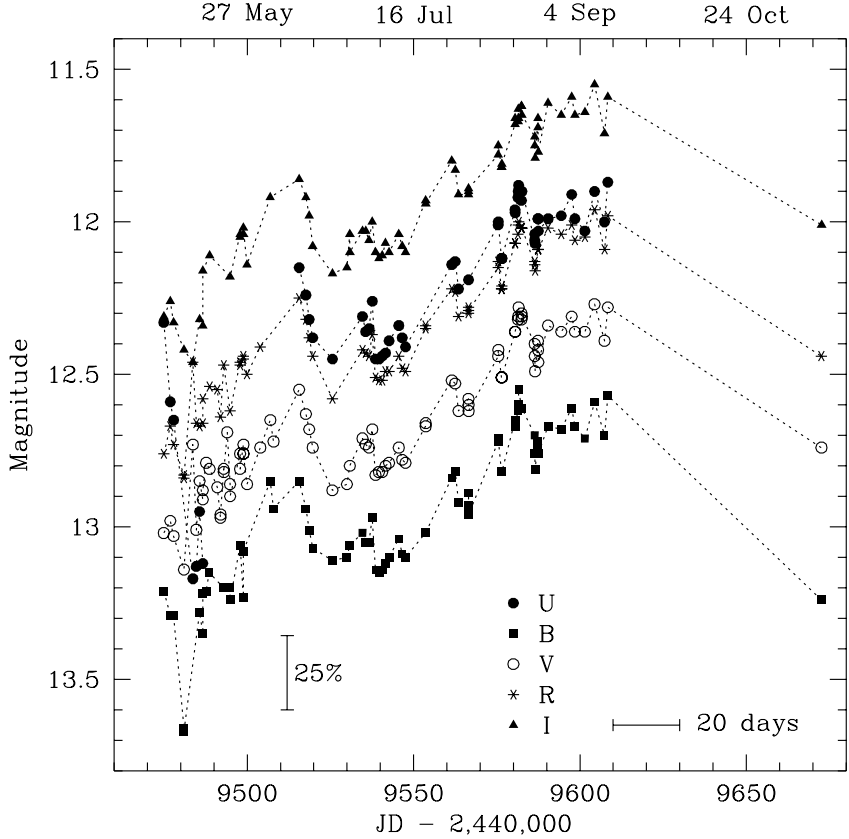


Fig. 6.— The complete optical light curves from 1994 April to November. Variations, from short-scale flickering ( $\sim 0.2$  mag in several days) to the longer-term trends, are of similar amplitude at all wavebands with no measurable lags. Uncertainties are the size of the points or smaller (they range from  $\lesssim 0.01$  to  $\sim 0.08$  mag, with 0.01 mag being typical). A time scale bar is shown for comparison with the other figures. The lines have been added to guide the eye only.

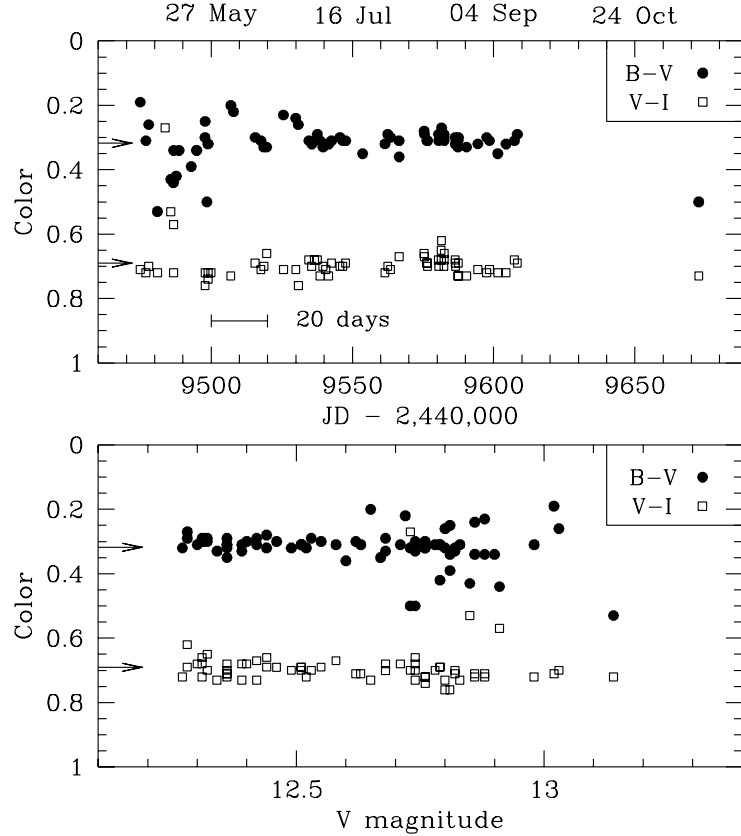


Fig. 7.— The  $B - V$  (solid circles) and  $V - I$  (open squares) colors for PKS 2155–304 as a function of time (*Top panel*) and  $V$  magnitude (*Bottom panel*). The largest color variations occur when the source is faint ( $V \gtrsim 12.7$ ). Average colors are  $\langle B - V \rangle = 0.32 \pm 0.02$  mag,  $\langle V - I \rangle = 0.69 \pm 0.01$  mag, and are marked with the arrows. The magnitudes used to calculate the colors were obtained simultaneously or nearly so (within  $\lesssim 10$  minutes in most cases).

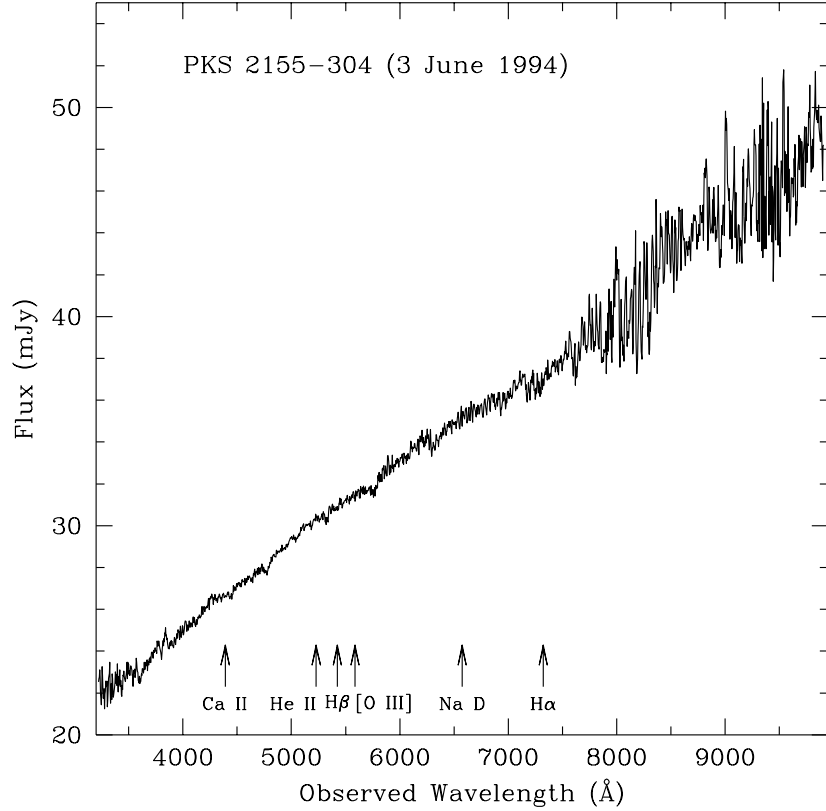


Fig. 8.— The optical spectrum of PKS 2155–304 from Lick (MJD 9506.9875). A power law with index  $\alpha = -0.71 \pm 0.02$  (where  $F_\nu \propto \nu^\alpha$ ) is a good representation of the spectrum, which is featureless to an equivalent width limit of  $\sim 1$  Å (or even 0.5 Å in most places). Typical features, if present at  $z = 0.116$ , would be at the locations marked. The high frequency oscillations most noticeable redward of 7500 Å are produced by incompletely flattened CCD interference fringes.

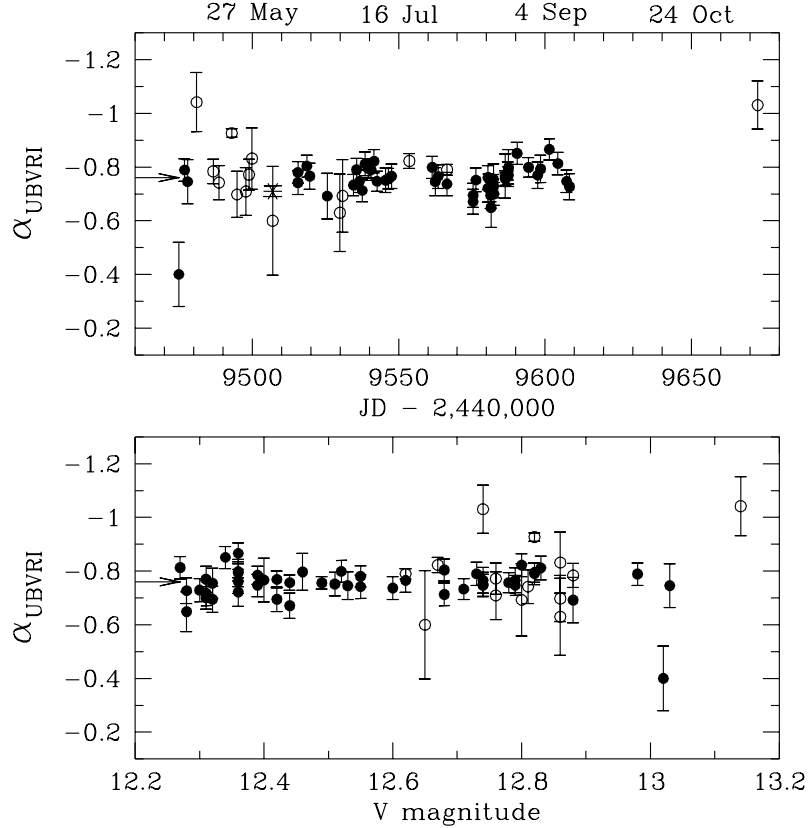


Fig. 9.— *Top panel*: Slope of the total flux energy distribution derived from fits ( $F_\nu \propto \nu^\alpha$ ) to five simultaneous  $UBVRI$  measurements (filled circles) and three or four simultaneous measurements (open circles). The average slope is  $\langle \alpha_{UBVRI} \rangle = -0.76 \pm 0.03$  (arrow). The asterisk is the slope from the Lick spectrum. *Bottom panel*: Same as above, but as a function of  $V$ -band magnitude. There is a very slight steepening of the spectrum with increasing magnitude, although this is not significant.

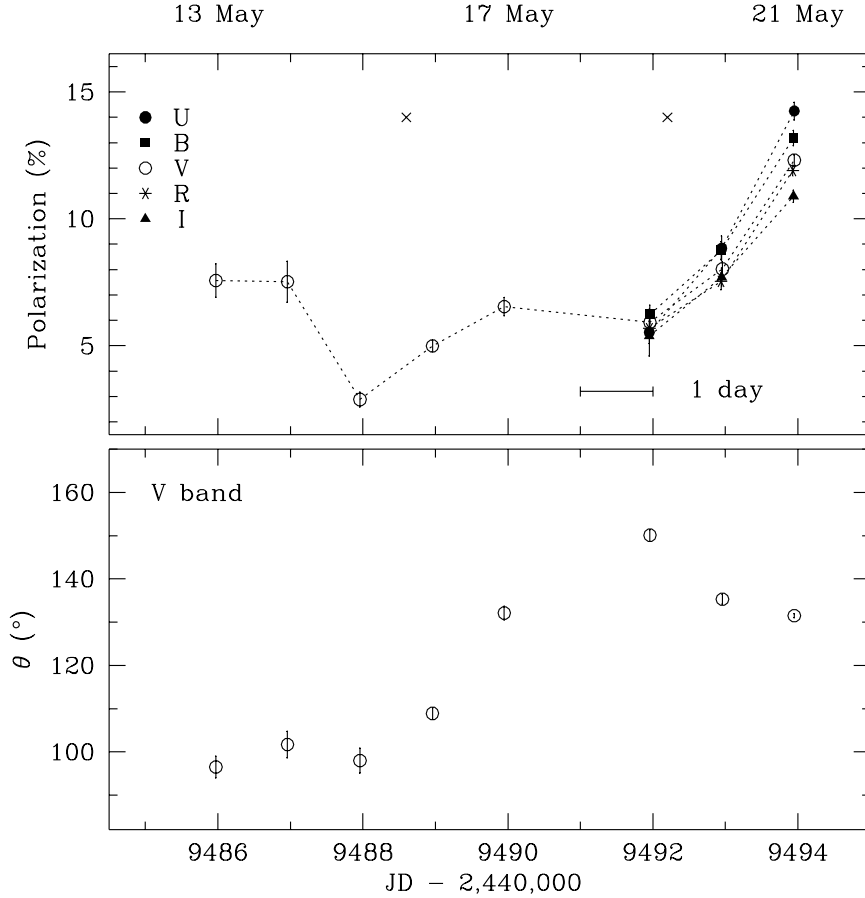


Fig. 10.— *Top panel:* The polarization light curves from 1994 May (Mt. Lemmon, Arizona). The increase in polarization after MJD 9492 occurs at all wavebands, and the wavelength dependent polarization is obvious. The increases in polarization after MJD 9488 and 9492 occur at the same time as the ultraviolet flaring events, the start times of which are marked with an “X” (Urry et al. 1996). A time scale bar is shown for comparison with the other figures. The lines have been added to guide the eye only. *Bottom panel:* The polarization position angle for the V band. The preferred range is  $\sim 90^\circ$  -  $150^\circ$ .

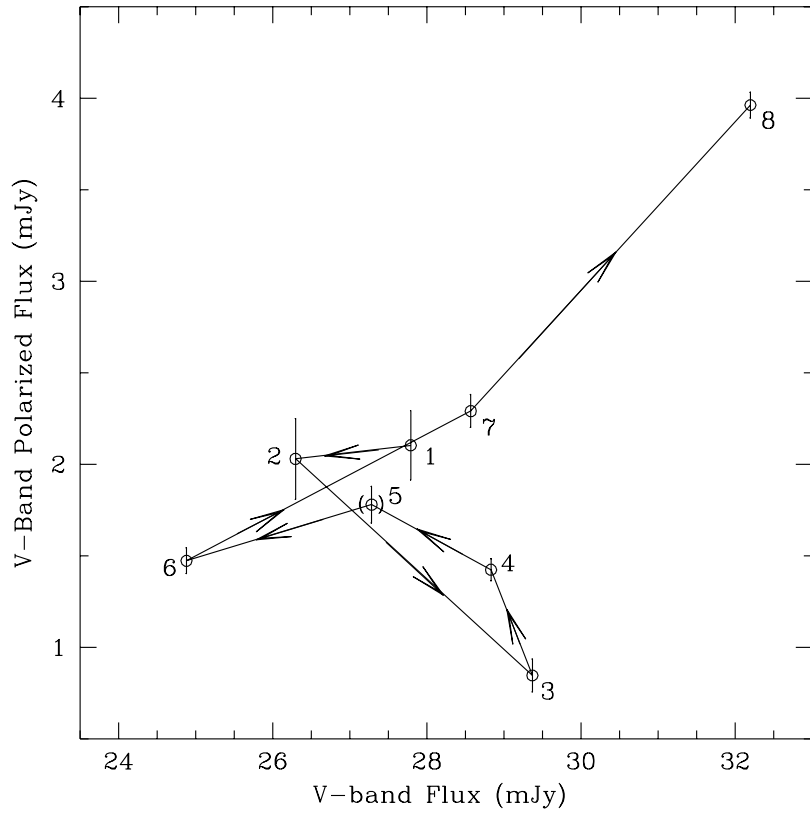


Fig. 11.— The polarized  $V$ -band flux versus  $V$ -band flux for 1994 May, numbered in chronological order. PKS 2155–304 both brightens and fades when the polarization increases. The two ultraviolet flaring events occurred after observations 3 and 6.